Science of the Total Environment 643 (2018) 451–459

Contents lists available at ScienceDirect

Science of the Total Environment

journal homepage: www.elsevier.com/locate/scitotenv

Geo-detection of factors controlling spatial patterns of heavy metals in urban topsoil using multi-source data

Tiezhu Shi [a,b], Zhongwen Hu [b,c], Zhou Shi [d], Long Guo [e], Yiyun Chen [f], Qingquan Li [b], Guofeng Wu [b,c,*]

[a] School of Architecture & Urban Planning, Shenzhen University, 518060 Shenzhen, China
[b] Key Laboratory for Geo-Environmental Monitoring of Coastal Zone of the National Administration of Surveying, Mapping and GeoInformation, Shenzhen Key Laboratory of Spatial Smart Sensing and Services, Shenzhen University, 518060 Shenzhen, China
[c] College of Life Sciences and Oceanography, Shenzhen University, 518060 Shenzhen, China
[d] Institute of Applied Remote Sensing and Information Technology, College of Environmental and Resource Sciences, Zhejiang University, 310058 Hangzhou, China
[e] College of Resources and Environment, Huazhong Agricultural University, 430070 Wuhan, China
[f] School of Resource and Environmental Sciences, Wuhan University, 430079 Wuhan, China

HIGHLIGHTS

- Heavy metals in topsoil are tracers of environmental contamination in urban area.
- Controlling factors of heavy metals reflect its pollution sources.
- Remote sensing provides convenient data to extract environmental factors.
- Geodetector explores factors controlling the spatial patterns of heavy metals.

GRAPHICAL ABSTRACT

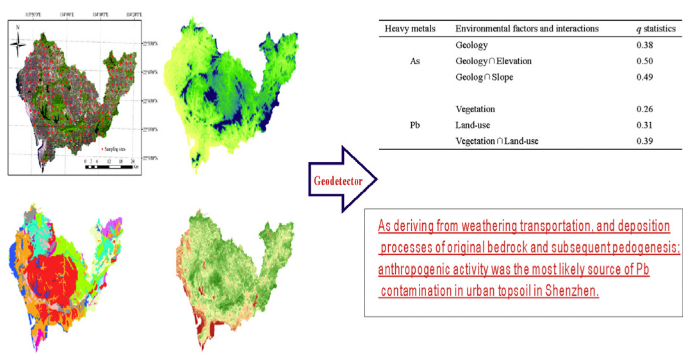

ARTICLE INFO

Article history:
Received 16 May 2018
Received in revised form 14 June 2018
Accepted 18 June 2018
Available online xxxx

Editor: F.M. Tack

Keywords:
Soil heavy metal contamination
CLORPT model
Anthropological activity
Geology
Remote sensing data

ABSTRACT

Heavy metal contamination has become a serious and widespread problem in urban environment. Understanding its controlling factors is vital for the identification, prevention, and remediation of pollution sources. This study aimed to identify the factors controlling heavy metal accumulation in urban topsoil using the geodetector method and multiple data sources. Environmental factors including geology, relief (elevation, slope, and aspect), and organism (land-use and vegetation) were extracted from a geological thematic map, digital elevation model, and time-series of Landsat images, respectively. Then, the power of determinant (q) was calculated using geodetector to measure the affinity between the environmental factors and arsenic (As) and lead (Pb). Geology was the dominant factor for As distribution in the this study area; it explained 38% of the spatial variation in As, and nonlinear enhancements were observed for the interactions between geology and elevation ($q = 0.50$) and slope ($q = 0.49$). Land-use and vegetation bi-enhanced each other and explained 39% of the spatial variation in Pb. These results indicated that geology and relief were the factors controlling the spatial distribution of As, and organism factors, especially anthropogenic activities, were the factors controlling the spatial distribution of Pb in the study area. As was derived from weathering transportation, and deposition processes of original bedrock and

* Corresponding author at: Key Laboratory for Geo-Environmental Monitoring of Coastal Zone of the National Administration of Surveying, Mapping and GeoInformation, Shenzhen Key Laboratory of Spatial Smart Sensing and Services, Shenzhen University, 518060 Shenzhen, China.
E-mail address: guofeng.wu@szu.edu.cn (G. Wu).

https://doi.org/10.1016/j.scitotenv.2018.06.224

subsequent pedogenesis, and anthropogenic activity was the most likely source of Pb contamination in urban topsoil in Shenzhen. Moreover, geodetector provided evidence to explore the factors controlling spatial patterns of heavy metals in soils.

1. Introduction

Urban regions are one of the most important places for human society and economic activities. According to the projections of the United Nations Population Division, the number of urban inhabitants in the developing world is likely to increase to 3.90 billion by 2030 and to 5.26 billion by 2050 (Montgomery, 2008). The growing population will introduce extreme pressures on urban ecological environments because some intensive human activities which involve industrial wastes, vehicle emissions, and household garbage generate a large number of contaminants, including heavy metals, polycyclic aromatic hydrocarbons, and polychlorinated biphenyls (Luo et al., 2012; Tang et al., 2005). These contaminants are mainly concentrated in urban topsoil (0–20 cm), especially heavy metals (Wang, 2009). For example, mineral and energy consumption by industries and transportation is accompanied by the release of heavy metals in fossils; these heavy metals enter the atmosphere through engine exhaust and factory emissions and fall to the ground under the influence of gravity or rainfall, and finally accumulate in urban topsoil. Therefore, heavy metals in topsoil have been shown to be useful tracers of environmental contamination in urban area (Manta et al., 2002).

Urban soil, a type of anthrosol, is frequently characterized by strong spatiotemporal heterogeneity because it mixes various inputs of exogenous materials from human activities with original soil materials (Morel and Heinrich, 2008). Soil surveys and research have been focused on agricultural and forest regions in order to adapt to the increasing demands for food and fiber of the growing global population, and urban soil has been neglected (Lu et al., 2012). Since the 1990s, the important and complex influences of urban soil on the ecological environment have been gradually recognized, and strong interests in urban and suburban soils have appeared. In 1998, the working group of Soils in Urban, Industrial, Traffic and Mining Areas was launched at the 16th World Congress of Soil Science in Montpellier, France. It aimed to advance the study of functions, status and restoration of urban soil, as well as its role in the evolution of urban ecosystems (Dickinson et al., 2013). Recently, given its threats to urban ecosystems, heavy metal contamination in urban soil has received increasing attention from soil and environment scientists.

Heavy metals threaten the heath of humans and urban ecosystems through wind, water, or plant trajectories. For instance, heavy metals can be carried by dust under the impact of wind, and can further enter and pose risks to humans through inhalation (Wang, 2009). Furthermore, heavy metals in polluted soils tend to be more mobile than those in unpolluted soils, therefore, heavy metals in urban soil may cause surface- and ground-water contamination (Wilcke et al., 1998). Approximately 65% of all Chinese cities exhibit high or extremely high levels of heavy metal contamination (Wei and Yang, 2010). Thus, there is an urgent need to understand their spatial patterns and controlling factors, which are vital for the identification, prevention, and remediation of pollution sources.

The CLORPT model is widely employed to explore the spatial patterns and controlling factors of soil properties. It regards soil as the product of the joint action of multiple environmental factors, including climate (cl), organisms (o), relief (r), parent material (p), and time (t) (Jenny, 1941), namely $S = f(cl, o, r, p, t)$. Climate factors include rainfall, temperature, and solar radiation; organisms include vegetation cover and types, land-use, and anthropological activities; relief refers to topography, such as slope, aspect, elevation, and slop angle; parent material, like rock type, is the original supply of soil mineral elements; and time is often a theoretical or hypothetical span for soil development. Natural and anthropogenic factors all play important roles in the formation of topsoil; therefore, the spatial patterns of soil heavy metals in urban topsoil are affected by not only parent material and soil forming processes, but also anthropogenic activities (Zhang, 2006). Many studies have confirmed that heavy metal contamination in soil is closely linked with multiple environmental factors, such as parent material, relief, and organisms (Bou Kheir et al., 2014; Liu et al., 2016; Qiu et al., 2015; Wilford et al., 2016).

Historical surveying data are usually adopted to extract environmental factors for the spatial analysis of soil heavy metals. For example, Bagheri et al. (2015) derived relief factors, including slope, aspect, and elevation, from a digital elevation model (DEM) at 10 m spatial resolution. Bou Kheir et al. (2014) and Wilford et al. (2016) employed geological maps to extract parent material factors to further explore their spatial association with soil heavy metals. Moreover, remotely sensed data, such as MODIS (Moderate Resolution Imaging Spectroradiometer), SPOT (satellite for observation of Earth), and IKONOS satellite images, are frequently applied to obtain vegetation indexes, land-use, and other organism factors (Huo et al., 2010; Wilford et al., 2016). ASTER (Advanced Space-borne Thermal Emission and Reflectance Radiometer), with an adopted optical stereo-technique, offers DEM data with a spatial resolution of 30 m. Based on ASTER data, Wilford et al. (2016) obtained multiple relief factors using digital terrain analysis techniques. Compared with historical surveying data, remotely sensed data are easier to access, cheaper, and timelier.

Remotely sensed images are often used to generate vegetation indexes and land-use information (Huo et al., 2010; Wilford et al., 2016); however, the time-varying traits of these environmental factors are not considered. Moreover, land-use and vegetation indexes change over time, especially in rapidly changing urban environments. Using images from a specific time may not reflect the effects of temporal variation in these factors on the accumulation of soil heavy metals. The Landsat series provides image records of the Earth's surface for more than four decades, and these images are suitable for extracting long term vegetation indexes and land-use information.

Principal component analysis (PCA) and cluster analysis (CA) are applied to assist in the identification of environmental factors controlling heavy metal accumulation (Chen et al., 1997; Guo et al., 2012; Lee et al., 2006; Li et al., 2004; Ordonez et al., 2003; Sun et al., 2013). PCA and CA classify heavy metals into different categories, and the most likely pollutant sources, such as parent materials or anthropogenic activities, are concluded by experience for each category. Another method to analyze controlling factors is based on the statistical relationship between environmental factors and heavy metals (Lin et al., 2002; Navas and Machin, 2002). However, the relationships among the spatial patterns of heavy metals and environmental factors are not taken into consideration in PCA, CA, or correlation analysis.

A geographical detector method, namely geodetector, may be a better choice for exploring the factors controlling heavy metal accumulation in urban topsoil. Geodetector is based on the spatial stratified heterogeneity of geographical phenomena; its key underlying assumption is that if a geographical factor A is controlled by another geographical factor B, then B will exhibit a spatial distribution similar to that of A (Luo et al., 2015; Wang et al., 2010; Wang et al., 2016). Geodetector has been applied to analyze the factors controlling the spatial patterns of various geographical phenomena. For instance, Luo et al. (2015) employed geodetector to identify the dominant factors of dissection

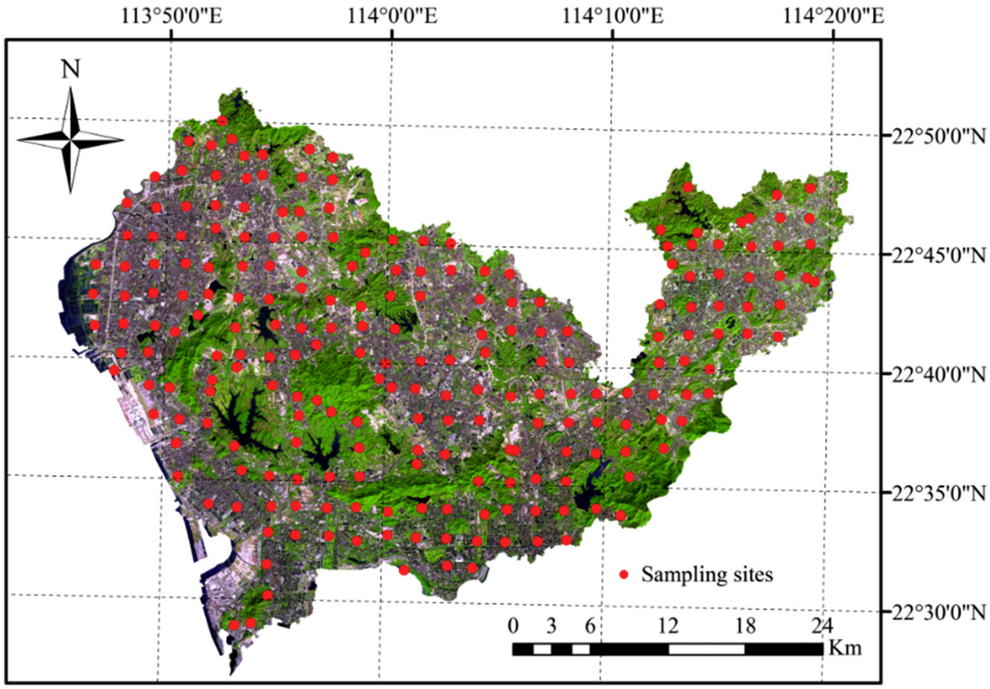

Fig. 1. Study area and sampling locations.

density over the entire conterminous United States, and Li et al. (2013) applied geodetector to investigate the spatial relationship between planting patterns and residual fluoroquinolones in soil.

Given the importance of heavy metal contamination in urban topsoil, this study aimed to identify the factors controlling heavy metal accumulation using geodetector and multiple data sources, especially time-series remotely sensed data. The results of this study are expected to reveal the internal regularities affecting the spatial pattern of heavy metals in urban topsoil, and to provide a geo-statistical way to explore their factors controlling these spatial patterns by combining geographical information science and remote sensing methods.

2. Materials and methods

2.1. Study area

Shenzhen (113°46′E to 114°37′E, 22°27′N to 22°52′N), which is located in the south of Guangdong Province, China, has a subtropical maritime climate with an average annual temperature of 22.4 °C and a mean annual precipitation of 1993.3 mm. Shenzhen holds various landform types, including plateaus, hills, and flood plains. Until 2016, four natural reserves have been established to protect mangroves, wetlands, and rare species. According to the Shenzhen Statistical Yearbook, there were approximately 11.37 million inhabitants in Shenzhen in 2016. Monitoring the heavy metal contamination in Shenzhen topsoil is vital for the sustainable development of the city ecosystem and the health of local citizens. Moreover, due to its low intensity of human activities before the Chinese economic reform, Shenzhen is a suitable representation of Chinese cities to explore environmental stress caused by rapid urbanization and industrialization since 1980.

2.2. Soil sampling

This study concentrated on the Baoan, Guangming, Nanshan, Futian, Luohu, Longhua, and Longgang districts of Shenzhen, in which most inhabitants live. The study area was divided into regular grids of 2 × 2 km for sampling, and a sampling site was randomly selected in each grid. The geographical coordinates of sampling sites were recorded using a global positioning system receiver, and information on land-use, vegetation cover, and landform were also recorded. A total of 221 topsoil samples were collected in November 2016 (Fig. 1), and artificial deposits, such as rubbles, concrete debris, and wastes, were avoided. Approximately 1.5 kg of topsoil (0–20 cm) were collected during five sampling campaigns (Shi et al., 2013) after removing plant residues, roots, and stones. The collected soil samples were kept in polyethylene bags and brought to a laboratory for heavy metal content analysis.

2.3. Soil heavy metal measurement

After air-drying at 20–26 °C for three days, the collected soil samples were ground with an agate mortar and sieved through a 100-mesh grid sieve (0.15 mm) to remove stones and coarse materials. In this study,

Table 1
Environmental factors for analyzing controlling factors of soil heavy metals.

Environmental factors		Data source	links
Organism	Vegetation Land-use	Landsat images	https://glovis.usgs.gov
Relief	Elevation, slope, and aspect	ASTER DEM	http://www.gscloud.cn
Parent material, time	Geology	Geological thematic map	http://www.szpl.gov.cn

Table 2
Descriptive statistics of arsenic (As) and lead (Pb) of soil samples (mg kg^{-1})[a].

	Minimum.	Maximum	Mean	Median	Skewness	S.D.
As	0.67	173.09	12.25	6.57	5.12	19.26
Pb	6.63	290.35	62.09	51.62	2.36	41.17

[a] S.D. is standard deviation.

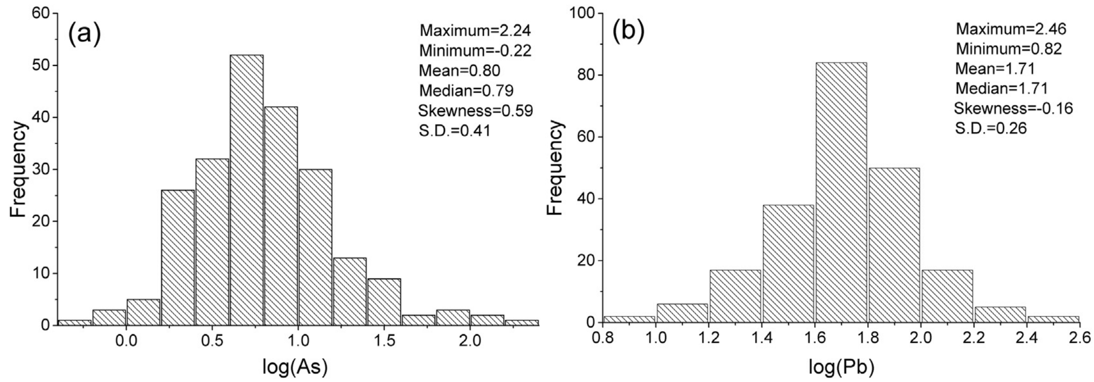

Fig. 2. Frequency distributions of logarithmically transformed soil As (a) and Pb (b) contents; S.D. is standard deviation.

arsenic (As) and lead (Pb) were selected to explore the application of geodetector for identifying controlling factors from multiple environmental factors. The soil As content was determined using hydride generation atomic fluorescence spectrometry, and the Pb content was measured using an atomic absorption flame spectrometer (Guo et al., 2009).

2.4. Environmental factors

Landsat images covering the study area in 1988, 1994, 1999, 2004, 2008, 2013 and 2016 (Table S1, downloaded from https://glovis.usgs.gov) were used to extract time-series information on organism factors, including land-use and vegetation. All images were captured in winter to keep the images cloud-free and to ensure a similar growing status of vegetation among different years. The images were geometrically and radiometrically corrected, and then further converted into reflectance values (Fig. S1) using the fast line-of-sight atmospheric analysis of spectral hypercube (Adler-Golden et al., 1990). Time-series normalized difference vegetation index (NDVI) values were calculated from the image reflectance. Images were classified into three land features, namely water body, artificial object, and terrestrial vegetation, using an object-oriented support vector machine classifier (Hu et al., 2016). The training datasets for image classification were determined by visually interpreting the imagery.

We hypothesized that soil heavy metal accumulation might be affected by organism factors at a specific spatial scale. Therefore, the buffers of sampling locations with different radii (100, 200, 300, 400, and 500 m) were generated. In these buffers, the average values of NDVI (B_{NDVI}) and the artificial objects' areas (B_{Area}) were calculated. Finally, the averages of time series B_{NDVI} and B_{Area} were calculated for vegetation and land-use factors, respectively.

The 1:50,000 geological map of Shenzhen (Fig. S2a) was acquired from the Urban Planning Land and Resources Commission of Shenzhen Municipality (http://www.szpl.gov.cn), and it was georeferenced and clipped to fit the study area (Fig. S2b). In order to digitize this geological map for computer processing, the object-oriented support vector machine classifier for images classification was adopted to distinguish geological types (Hu et al., 2016). Relief information on surface topography, including elevation, slope, and aspect, was derived from DEM data (30 m) of ASTER (http://www.gscloud.cn). The environmental factors employed for controlling factor analysis are listed in Table 1.

2.5. Geographical detector method

The geographical detector method was developed to measure the spatially stratified heterogeneity of geographic variable *Y* (for example,

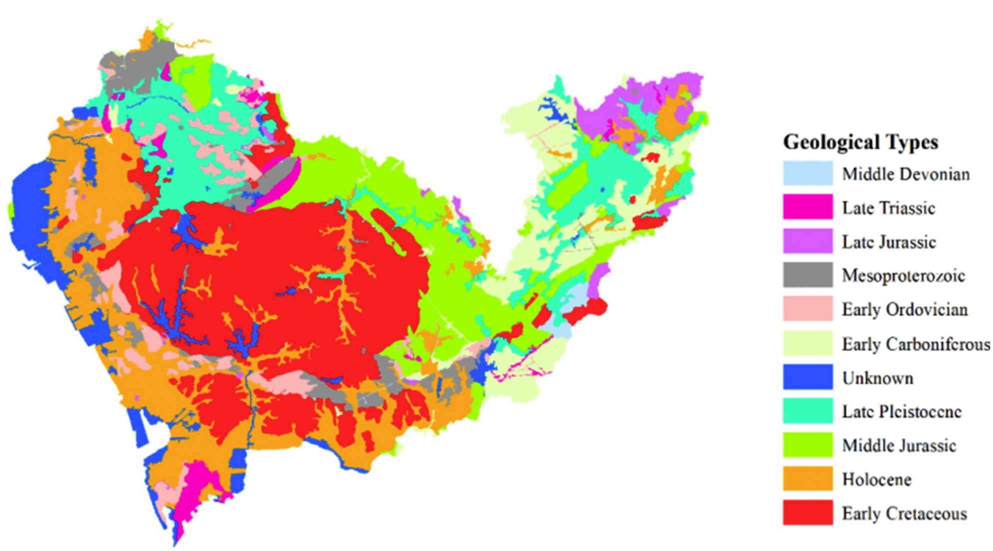

Fig. 3. Major geological types of study area. The Unknown type was caused by no investigations due to water coverage.

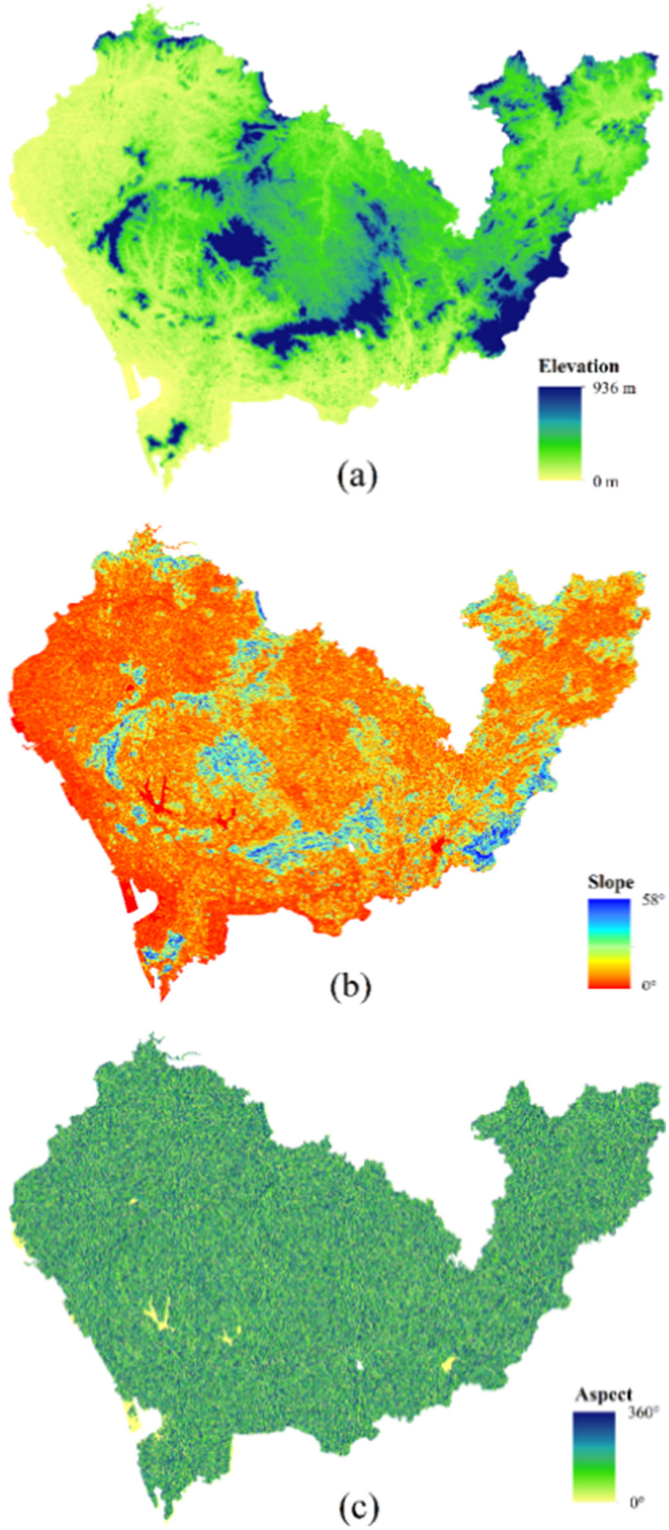

Fig. 4. Relief factors of surface topography, including elevation (a), slope (b) and aspect (c).

heavy metals in this study) and to explore how factor X explains the spatial pattern of Y. Formally, Y is composed of N samples, and X is stratified into L strata; stratum $h \in [1, 2, \ldots, L]$ is composed of N_h samples; y_i is the value of sample i in the whole sample population; and y_{hi} denotes the value of sample i in stratum h. The concept of spatially stratified heterogeneity is the q-statistic, which is defined as follows (Wang et al., 2016):

$$q = 1 - \frac{\sum_{h=1}^{L}\sum_{i=1}^{N_h}(y_{hi} - \overline{y}_h)^2}{\sum_{i=1}^{N}(y_i - \overline{y})^2} = 1 - \frac{\sum_{h=1}^{L} N_h \sigma_h^2}{N\sigma^2} = 1 - \frac{SSW}{SST} \tag{1}$$

where $\overline{y}_h = (1/N_h)\sum_{i=1}^{N_h} y_{hi}$ is the mean value of stratum h; $\overline{y} = (1/N)\sum_{i=1}^{N} y_i$ is the mean value of the population; $\sigma_h{}^2 = (1/N_h)\sum_{i=1}^{N_h}(y_{hi} - \overline{y_h})^2$ is the variance in stratum h; and $\sigma^2 = (1/N)\sum_{i=1}^{N}(y_i - \overline{y})^2$ is the variance in the population. *SSW* and *SST* denote the within sum of squares and total sum of squares, respectively (Wang et al., 2016; Wang and Xu, 2017).

For $q \in [0, 1]$, a higher value of q indicates a stronger spatially stratified heterogeneity of Y. When the strata are defined by factor X, q indicates that factor X can explain $100 \times q\%$ of the spatial pattern of Y. The factor X must be a categorical variable in calculating the q value. If factor X is a continuous variable, it needs to be categorized using expert knowledge or a categorization algorithm, such as equal interval, quantile, and k-means (Wang and Xu, 2017). The categorized levels depend on the improvement of the q value (Wang and Xu, 2017). In this study, the relief factors (elevation, slope, and aspect) and organism factors (vegetation and land-use factors) were categorized using the k-means method. Moreover, the number of categorized types and optimal buffers were determined by the maximum q value, and p value was used for the significance test (Wang et al., 2016).

Furthermore, an "interaction detector" was defined to assess the interaction between two different factors, namely X_1 and X_2, by comparing $q(X_1 \cap X_2)$ with $q(X_1)$ and $q(X_2)$. $X_1 \cap X_2$ indicates a new stratum created by overlaying factors X_1 and X_2 (Luo et al., 2015; Wang and Xu, 2017). If $q(X_1 \cap X_2) > q(X_1)$ or $q(X_2)$, then the two factors enhance each other; if $q(X_1 \cap X_2) > q(X_1)$ and $q(X_2)$, then the factors bi-enhance each other; and if $q(X_1 \cap X_2) > q(X_1) + q(X_2)$, then the two factors nonlinearly enhance each other. If the opposite of these formulas is true (e.g., $q(X_1 \cap X_2) < q(X_1)$ or $q(X_2)$), then the two factors weaken, bi-weaken, or nonlinearly weaken each other, respectively. If $q(X_1 \cap X_2) = q(X_1) + q(X_2)$, then the factors are independent of each other (Luo et al., 2015; Wang et al., 2010; Wang and Xu, 2017). The free software for executing this geographical detector method was downloaded from http://www.geodetector.org.

3. Results

3.1. Heavy metals

The descriptive statistics for As and Pb are shown in Table 2. As and Pb contents varied in the ranges of 0.67–173.09 and 6.63–290.35 mg kg^{-1} with average values of 12.25 and 62.09 mg kg^{-1}, respectively, and showed positive skew distributions with skewness values of 5.12 and 2.36. Therefore, these content values were logarithmically (log(10)) transformed (Fig. 2) to improve their normal distributions. According to the Chinese Environmental Quality Standard for Soils (GB 15618–1995) (Chen et al., 2016), 27% and 74% of these soil samples exceeded background levels for As and Pb, respectively. This suggests high As and Pb pollution risks in the study area in terms of soil environmental quality.

3.2. Environmental factors

Ten major geological types were diagnosed from thematic geological maps (Fig. 3), including Middle Devonian, Late Triassic, Late Jurassic, Mesoproterozoic, Early Ordovician, Early Carboniferous, Late Pleistocene, Middle Jurassic, Holocene and Early Cretaceous. The relief factors, including elevation, slope and aspect, are shown in Fig. 4. The elevation of this area ranges from 0 to 936 m, and the slope ranges from 0° to 58°.

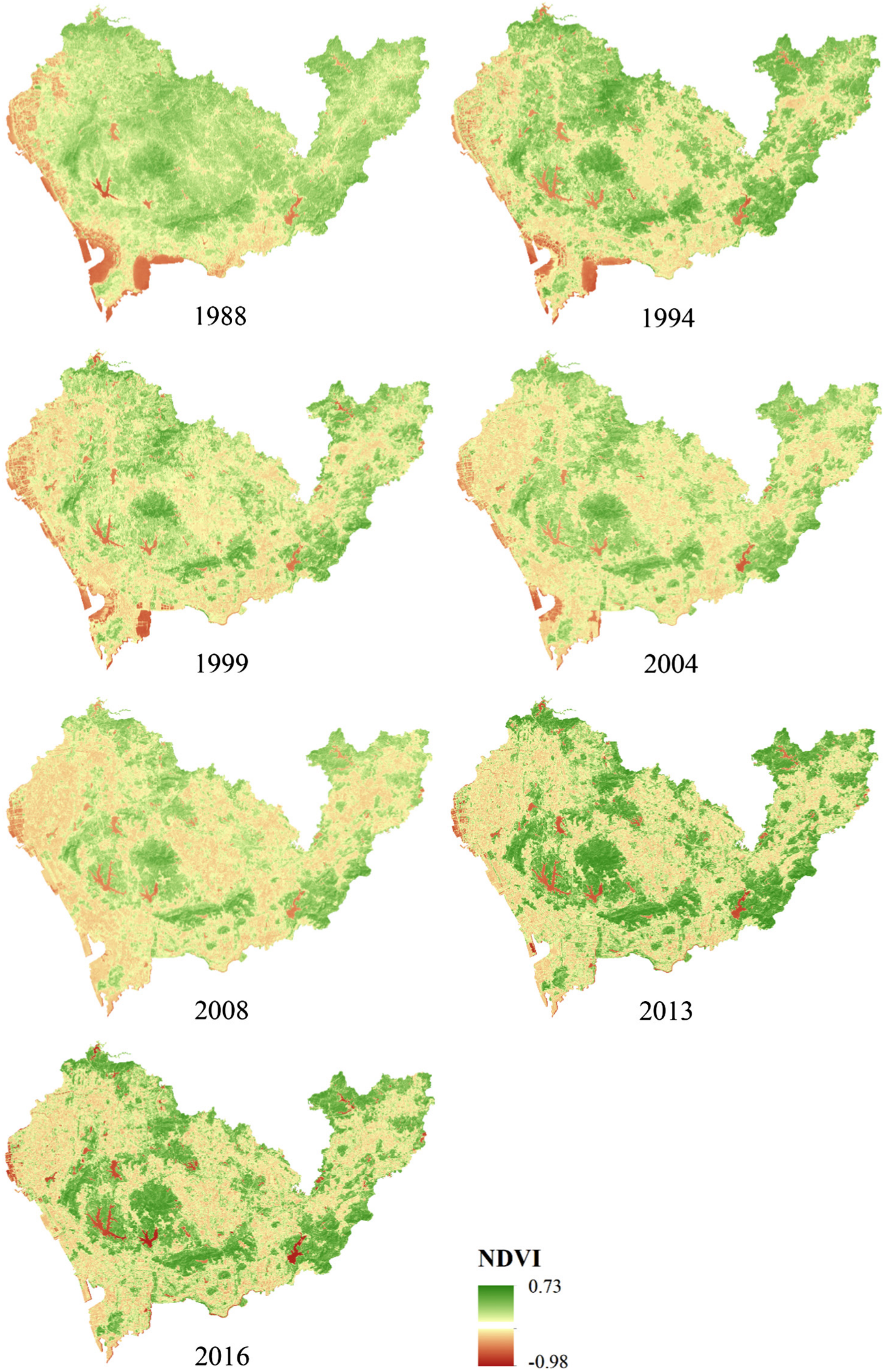

Fig. 5. Time-series normalized difference vegetation index (NDVI) of study area.

The time-series of NDVI and land features are shown in Figs. 5 and 6, respectively. Vegetation coverage decreased and artificial construction land increased continuously during 1988 to 2016. Considering that the optimal buffers for vegetation and land-use factors were 200 m, the correlation coefficients of log(Pb) against vegetation and land-use factors were 0.56 and −0.46, respectively (Fig. 7). This demonstrated that the Pb contents in urban soil generally increased with the intensification of human activities and decreased with increasing vegetation coverage.

3.3. *q* statistics

All environmental factors in Table 1 and their interactions were considered in *q* statistics for As and Pb. For As, environmental factors, including aspect, land-use, and vegetation did not pass the significance test at a significance level of 0.05. The *q* statistic results indicated that the geological factor was the dominant factor for As distribution in the study area, and it explained 38% of the spatial variation in As

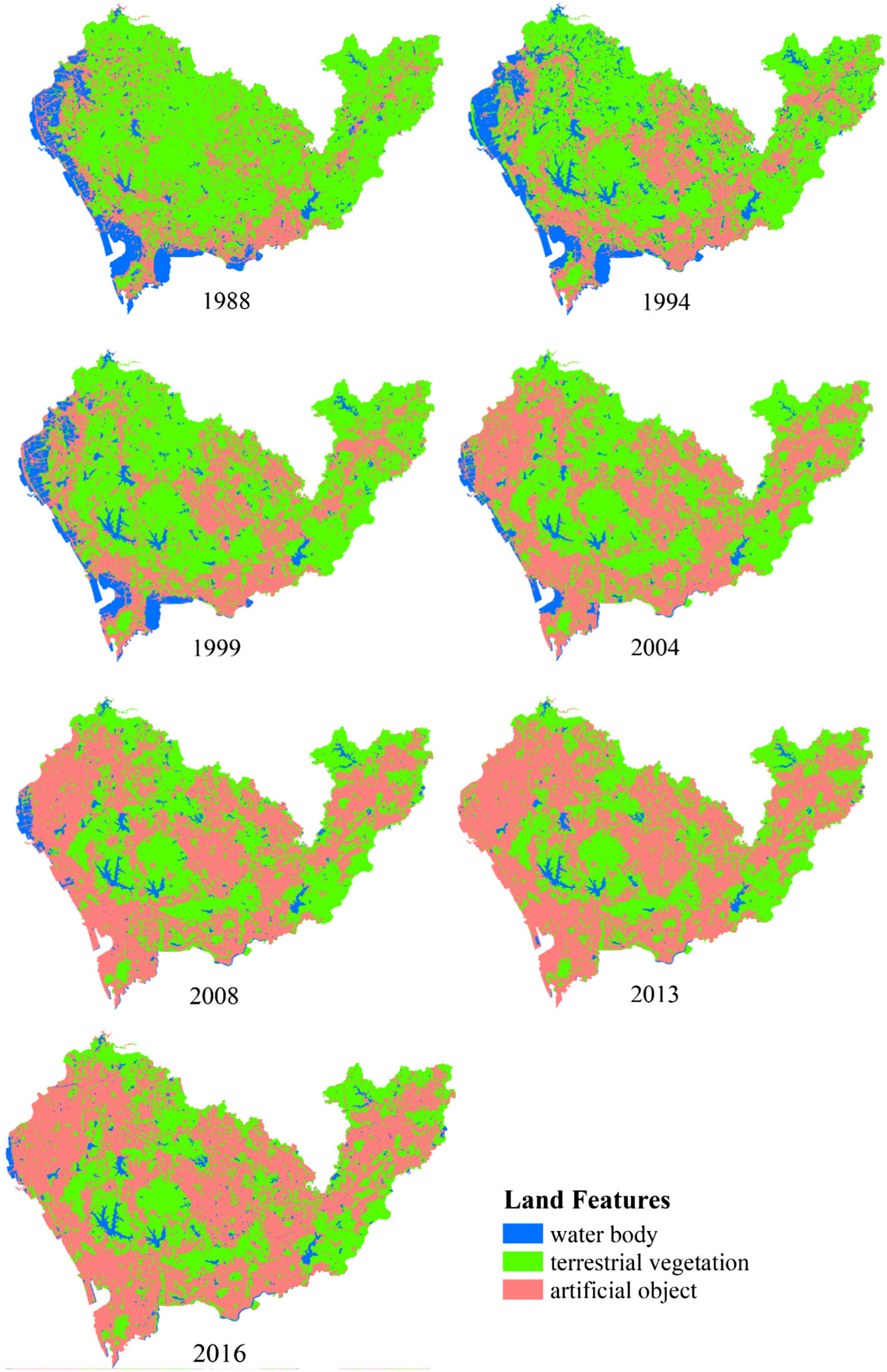

Fig. 6. Land features change from 1988 to 2016 in study area.

(Table 3). The elevation and slope were classified into five and three categories by k-means, respectively. Nonlinear enhancements were observed for the interactions between geology and elevation ($q = 0.50$) and slope ($q = 0.49$), which indicated that geology and relief were the factors controlling the spatial pattern of As.

For Pb, geological and relief factors (elevation, slope, and aspect) did not pass the significance test at a significance level of 0.05. The vegetation and land-use were categorized into five and eight types using k-means, and they explained 31% and 26% of the spatial pattern of Pb in urban topsoil, respectively (Table 3). Moreover, the vegetation and land-use bi-enhanced each other and explained 39% of the spatial variation in Pb, which indicated that organism factors, especially anthropogenic activities, were the factors controlling for the spatial pattern of Pb in the study area.

4. Discussion

In this study, geodetector was employed to explore the factors controlling heavy metal accumulation in urban topsoils. Compared with PCA and CA, geodetector provided more convincing evidence to explain

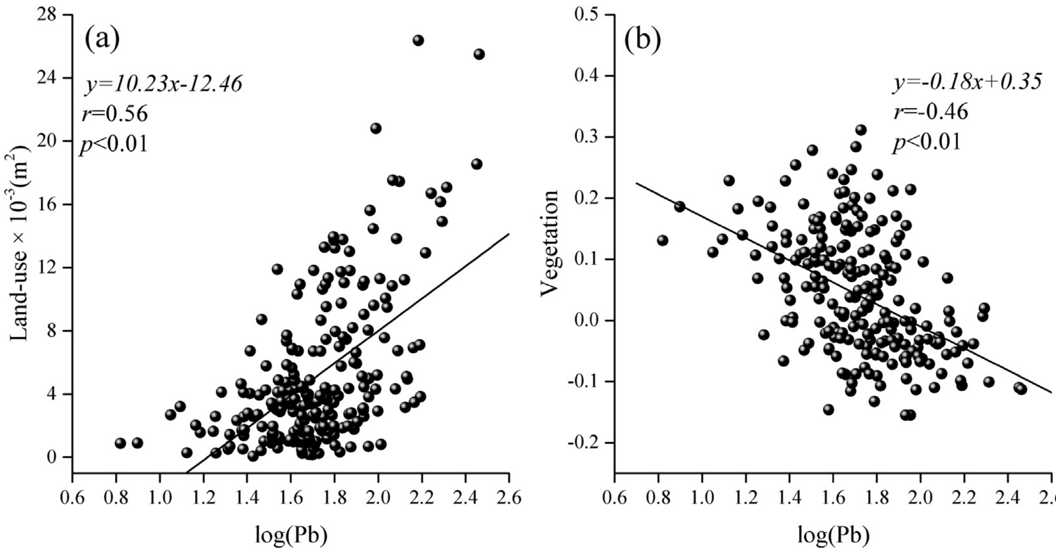

Fig. 7. Pearson correlation between logarithmically (log(10)) transformed lead (Pb) contents with vegetation and land-use factors.

controlling factors by measuring the consistency of their spatially stratified heterogeneity with heavy metals. Wang and Xu (2017) declared that the consistency of spatial distribution between two geographic variables was more difficult to obtain than linear correlation of the two variables. Therefore, compared with Pearson correlation analysis, geodetector offered stronger statistics to reveal the causal relationship between independent and dependent variables (Wang and Xu, 2017). Moreover, geodetector is designed for processing categorical variables, such as the geological type in this study, whereas Pearson correlation analysis is not suitable for processing this kind of data.

Multi-source data (geological thematic map, ASTER DEM, and Landsat images), remote sensing, and geographical information techniques were adopted to derive various environmental factors in this study. These data are usually free and available for most urban areas globally. Based on this fact, we believe that the technical approach proposed in this study could be applied to other urban regions to extract environmental factors and further to analyze the factors controlling the spatial distribution of heavy metal.

The spatial scale of environmental factors has not received full comprehension and emphasis in most studies (Huo et al., 2010; Wilford et al., 2016). We believe that the spatial scale of environmental factors is important in affecting heavy metal accumulation, and should be taken into account in calculating human activity factors. This point was supported by the result that the q values for land-use (Table S2) and vegetation factors (Table S3) increased with increasing buffer values up to 200 m. Moreover, there were significant correlations between land-use (Table S4) and vegetation factors (Table S5) employing different buffers, which might have been attributed to the spatial correlation of artificial object's area and NDVI. Therefore, we considered that the q value would be stabilized even when adopting larger buffer values (Tables S2 and S3). This result indicated that the spatial influence of heavy metal accumulations might be at a specific scale, such as about 200 m in this study.

Li et al. (2001) demonstrated that heavy metal concentrations in urban park soils were significantly related to the age of the parks, which might reflect the accumulation time of heavy metals. Therefore, in this study, a time series of Landsat images were used to reveal the dynamic change characteristics of land features and vegetation coverage. The changes might reflect the duration and intensity of human activities and their effects on the long-term accumulation of heavy metals in urban areas. Because of the lack of archive images or cloud cover of existed images, only Landsat images from 1988, 1994, 1999, 2004, 2008, 2013 and 2016 were chosen to extract the time series of organism factors. Due to the temporal correlation of artificial object's area and NDVI, there were significant correlations between neighboring annual B_{Area} (Fig. S3) and B_{NDVI} (Fig. S4) in the 200 m buffers derived from the time-series Landsat images. However, if data are available, then Landsat images with higher temporal resolution are preferred to reflect the detailed changes in land feature and NDVI.

Analyzing the controlling factors of heavy metals helps to differentiate the pollution sources for various heavy metals and to assess their risks. In this study, climate factors were not considered as potential controlling factors because the climate was generally the same for the whole Shenzhen. Therefore, geology (parent material and time), relief, and organism factors were employed for q analysis.

We found that geology and relief factors played major roles in the spatially stratified heterogeneity of As in the study area, which demonstrated that the As in urban soils was derived from weathering transportation, and deposition processes of original bedrock and subsequent pedogenesis. This result was consistent with the finding by Guo et al. (2012), who indicated that spatial distribution of As in urban soils is mainly controlled by soil parent materials. Moreover, Navas and Machin (2002) also supported the finding that soil As originated from parent materials because they found that the soils developed on sedimentary rocks had the lowest As contents, while the soils overlying

Table 3
Environmental factors and factor interactions with q values.

Heavy metals	Environmental factors and interactions	q statistics
As	Geology	0.38
	Elevation	0.05
	Slope	0.05
	Aspect	0.01
	Vegetation	0.00
	Land-use	0.00
	Geology∩Elevation	0.50
	Geology∩Slope	0.49
Pb	Geology	0.02
	Elevation	0.00
	Slope	0.00
	Aspect	0.00
	Vegetation	0.26
	Land-use	0.31
	Vegetation∩Land-use	0.39

metamorphic and igneous rocks had the highest As contents. In this study, residents living in regions with soils from the Late Pleistocene (Table S6, mean = 1.31, standard deviation = 0.28) face higher risks of As contamination.

This study also demonstrated that anthropogenic activity was a significant source of Pb pollution in topsoils. Therefore, anthropogenic sources, such as industrial wastes, vehicle emissions, and household garbage, were the most likely sources of Pb contamination in urban topsoil in Shenzhen. This result was consistent with the widely accepted point that high contents of Pb in urban topsoil are associated with the atmospheric deposition of vehicle emissions resulting from the use of leaded gasoline (Imperato et al., 2003; Saby et al., 2006). Despite the ban on Pb additives in gasoline in China, followed by a rapid decrease in Pb levels in the atmosphere, the contents of Pb accumulated in urban topsoils will remain high (Guo et al., 2012), and may poison children via a soil hand mouth pathway (Imperato et al., 2003).

5. Conclusions

This study explored the factors controlling heavy metal accumulation in urban topsoil using a geographical detector method and multiple data sources. The most important conclusions were as follows.

(1) Geodetector provided evidence to explore the factors controlling the spatial patterns of heavy metals in soils.
(2) As in urban topsoil within Shenzhen was derived from weathering transportation, and deposition processes of original bedrock and subsequent pedogenesis.
(3) Anthropogenic pollutants, such as industrial wastes, vehicle emissions, and household garbage, were the most likely source of Pb contamination in urban topsoil in Shenzhen.

Acknowledgments

This study was supported by the National Natural Science Foundation of China (No. 4170010438), the Basic Research Program of Shenzhen Science and Technology Innovation Committee (No. JCYJ20170302144323219).

Appendix A. Supplementary data

Supplementary data to this article can be found online at https://doi.org/10.1016/j.scitotenv.2018.06.224.

References

Adler-Golden, S.M., Matthew, M.W., Bernstein, L.S., Levine, R.Y., Berk, A., Richtsmeier, S.C., Acharya, P.K., Anderson, G.P., Felde, G., Gardner, J., Hoke, M., Jeong, L.S., Pukall, B., Mello, J., Ratkowski, A., Burke, H.H., 1990. Atmospheric correction for short-wave spectral imagery based on MODTRAN4. Proceedings of SPIE-the International Society for Optical Engineering. Vol. 3753, pp. 61–69.
Bagheri, B.M., Martinez-Casasnovas, J.A., Salehi, M.H., Mohammadi, J., Esfandiapoor, B.I., Toomanian, N., Gandomkar, A., 2015. Digital soil mapping using artificial neural networks and terrain-related attributes. Pedosphere 25, 580–591.
Bou Kheir, R., Shomar, B., Greve, M.B., Greve, M.H., 2014. On the quantitative relationships between environmental parameters and heavy metals pollution in Mediterranean soils using gis regression-trees: the case study of Lebanon. J. Geochem. Explor. 147, 250–259.
Chen, T.B., Wong, J.W.C., Zhou, H.Y., Wong, M.H., 1997. Assessment of trace metal distribution and contamination in surface soils of Hong Kong. Am. J. Infect. Control 96, 61–68.
Chen, T., Chang, Q.R., Clevers, J.G.P.W., Kooistra, L., 2016. Identification of soil heavy metal sources and improvement in spatial mapping based on soil spectral information: a case study in Northwest China. Sci. Total Environ. 565, 155–164.
Dickinson, N., Morel, J.L., Shaw, R.K., Wessolek, G., 2013. Iuss suitma 6 international symposium 2011. J. Soils Sediments 13, 489–490.
Guo, J.H., Ma, H., Wang, S.F., 2009. Determination of arsenic in national standard reference soil and stream sediment samples by atomic fluorescence spectrometry (in Chinese). Rock Miner Anal. 28, 182–184.
Guo, G., Wu, F., Xie, F., Zhang, R., 2012. Spatial distribution and pollution assessment of heavy metals in urban soils from Southwest China. J. Environ. Sci. 24, 410–418.
Hu, Z.W., Li, Q.Q., Zou, Q., Zhang, Q., Wu, G.F., 2016. A bilevel scale-sets model for hierarchical representation of large remote sensing images. IEEE Trans. Geosci. Remote. 54, 7366–7377.
Huo, X.N., Li, H., Sun, D.F., Zhang, W.W., Zhou, L.D., Li, B.G., 2010. Spatial autogression model for heavy metals in cultivated soils of Beijing (in Chinese). Trans. CSAE. 26, 78–82.
Imperato, M., Adamo, P., Naimo, D., Arienzo, M., Stanzione, D., Violante, P., 2003. Spatial distribution of heavy metals in urban soils of Naples city (Italy). Environ. Pollut. 124, 247–256.
Jenny, H., 1941. Factors of Soil Formation - a System of Quantitative Pedology. McGraw Hill Book Co, New York, USA.
Lee, C.S., Li, X.D., Shi, W.Z., Cheung, S.C., Thornton, I., 2006. Metal contamination in urban, suburban, and country park soils of Hong Kong: a study based on GIS and multivariate statistics. Sci. Total Environ. 356, 45–61.
Li, X.D., Poon, C.S., Liu, P.S., 2001. Heavy metal contamination of urban soils and street dusts in Hong Kong. Appl. Geochem. 16, 1361–1368.
Li, X.D., Lee, S.L., Wong, S., Shi, W.Z., Thornton, I., 2004. The study of metal contamination in urban soils of Hong Kong using a gis-based approach. Environ. Pollut. 129, 113–124.
Li, X.W., Xie, Y.F., Wang, J.F., Christakos, G., Si, J.L., Zhao, H.N., Ding, H.N., Li, J., 2013. Influence of planting patterns on fluoroquinolone residues in the soil of an intensive vegetable cultivation area in northern China. Sci. Total Environ. 458-460, 63–69.
Lin, Y.P., Teng, T.P., Chang, T.K., 2002. Multivariate analysis of soil heavy metal pollution and landscape pattern in Chuanghua county in Taiwan. Landsc. Urban Plan. 62, 19–35.
Liu, R., Wang, M., Chen, W., Peng, C., 2016. Spatial pattern of heavy metals accumulation risk in urban soils of Beijing and its influencing factors. Environ. Pollut. 210, 174–181.
Lu, Y., Gong, Z.T., Zhang, G.L., 2012. Characteristics and management of urban soils (in Chinese). Soil Environ. Sci. 11, 206–209.
Luo, X.S., Yu, S., Zhu, Y.G., Li, X.D., 2012. Trace metal contamination in urban soils of China. Sci. Total Environ. 421-422, 17–30.
Luo, W., Jasiewicz, J., Stepinski, T., Wang, J.F., Xu, C.D., Cang, X.Z., 2015. Spatial association between dissection density and environmental factors over the entire conterminous United States. Geophys. Res. Lett. 43, 692–700.
Manta, D.S., Angelone, M., Bellanca, A., Neri, R., Sprovieri, M., 2002. Heavy metals in urban soils: a case study from the city of Palermo (Sicily), Italy. Sci. Total Environ. 300, 229–243.
Montgomery, M.R., 2008. The urban transformation of the developing world. Science 319, 761–763.
Morel, J.L., Heinrich, A.B., 2008. Suitma-soils in urban, industrial, traffic, mining and military areas. J. Soils Sediments 8, 206–207.
Navas, A., Machin, J., 2002. Spatial distribution of heavy metals and arsenic in soils of Aragon (Northeast Spain): controlling factors and environmental implications. Appl. Geochem. 17, 961–973.
Ordonez, A., Loredo, J., De Miguel, E., Charlesworth, S., 2003. Distribution of heavy metals in the street dusts and soil of an industrial city in northern Spain. Arch. Environ. Contam. Toxicol. 44, 160–170.
Qiu, M., Li, F., Wang, Q., Chen, J., Yang, G., Liu, L., 2015. Driving forces of heavy metal changes in agricultural soils in a typical manufacturing center. Environ. Monit. Assess. 187, 1–14.
Saby, N., Arrouays, D., Boulonne, L., Jolivet, C., Pochot, A., 2006. Geostatistical assessment of Pb in soil around Paris, France. Sci. Total Environ. 367, 212–221.
Shi, T.Z., Cui, L.J., Wang, J.J., Fei, T., Chen, Y.Y., Wu, G.F., 2013. Comparison of multivariate methods for estimating soil total nitrogen with visible/near-infrared spectroscopy. Plant Soil 366, 363–375.
Sun, C.Y., Liu, J., Wang, Y., Sun, L., Yu, H., 2013. Multivariate and geostatistical analyses of the spatial distribution and sources of heavy metals in agricultural soil in Dehui, Northeast China. Chemosphere 92, 517–523.
Tang, L., Tang, X.Y., Zhu, Y.G., Zheng, M.H., Miao, Q.L., 2005. Contamination of polycyclic aromatic hydrocarbons (PAHs) in urban soils in Beijing, China. Environ. Int. 31, 822–828.
Wang, X.S., 2009. Accumulation-leaching Characteristics and Magnetic Proxies of Heavy Metals in Urban Topsoil. China Environmental Science Press, Beijing, China.
Wang, J.F., Xu, C.D., 2017. Geodetector: principle and prospective. Acta Geograph. Sin. 72, 116–134.
Wang, J.F., Li, X.H., Christakos, G., Liao, Y.L., Zhang, T., Gu, X., Zhang, X.Y., 2010. Geographical detectors-based health risk assessment and its application in the neural tube defects study of the Heshun region, China. Int. J. Geogr. Inf. Syst. 24, 107–127.
Wang, J.F., Zhang, T.L., Fu, B.J., 2016. A measure of spatial stratified heterogeneity. Ecol. Indic. 67, 250–256.
Wei, B., Yang, L., 2010. A review of heavy metal contamination in urban soils, urban road dusts and agricultural soils from China. Microchem. J. 94, 99–107.
Wilcke, W., Muller, S., Kanchanakool, N., Zech, W., 1998. Urban soil contamination in Bangkok: heavy metal and aluminium partitioning in topsoils. Geoderma 86, 211–228.
Wilford, J., de Caritat, P., Bui, E., 2016. Predictive geochemical mapping using environmental correlation. Appl. Geochem. 66, 275–288.
Zhang, C., 2006. Using multivariate analyses and GIS to identify pollutants and their spatial patterns in urban soils in Galway, Ireland. Environ. Pollut. 142, 501–511.